International Journal of Applied Engineering Research ISSN 0973-4562 Volume 13, Number 8 (2018) pp. 5-11

Numerical assessment of suitability of phase-change materials in a concentric PCM-module for thermal storage applications

Sumer Bharat Dirbude
Assistant Professor, Department of Mechanical Engineering,
National Institute of Technology Delhi,
Institutional Area, Narela, Delhi-40, India.

Dnyaneshwar Shantiram Shelke
M. Tech. student, Department of Mechanical Engineering,
National Institute of Technology Delhi,
Institutional Area, Narela, Delhi-40, India.

Abstract
Thermal heat storage devices based on latent-heat-based storage found to have the highest storage capacity of PCM ranging from 50-150 kWh/t with the heat transfer efficiency approximately between 75-90%. The available phase-change materials (PCMs) range from metals to organic compounds. These materials not only vary in their thermo-physical properties, but also in their availability and cost. In this work, 2D, unsteady, and laminar numerical simulations using ANSYS-Fluent with the enthalpy-porosity formulation is performed with three PCMs, viz., gallium (pure metal), paraffin wax (organic compound) and sodium nitrate (pure inorganic compound) to study the melting during charging-phase in the concentric PCM-module. The vertical wall of the 2D-cavity is exposed to the stagnant heat transfer fluid at 590 K and other three walls are considered as insulated. The model is verified and numerical comparison between metal-based, and organic and inorganic compound-based PCM is made in this preliminary study, for the melting and heat-transfer behavior, availability and cost.
Keywords: Phase change materials, PCM module, Computational Fluid Dynamics, Solar energy
.

Introduction

Phase Change Material (PCM) based heat storage devices are nowadays preferred to store and deliver energy for heat and power applications [1, 2] as compared to the storage devices based on sensible heat. A reason is that the latent-heat based storage devices have higher heat storage capacities ranging from 50-150 kWh/t with the efficiency between 75-90% [3] based on the type of the PCM material used. They store and release heat at almost constant temperature, with storage capacity 5-14 times larger than that of the sensible heat storage devices [4]. The phase-change materials (PCMs) range from organic to eutectics to inorganic, for example, paraffin wax, salt hydrates, gallium, sodium nitrate, potassium nitrate, etc. Also, their thermo-physical properties and cost and availability vary from one PCM to another [4, 5]. It is quite conclusive that the heat transfer efficiency is less for the low (approximately in the range approx. 0.2-0.7 W/m K) thermal conductivity PCM [3, 4]. However, it is possible to improve the heat transfer performance, when low conductivity PCM is used, by using some intrusive or non-intrusive strategies.

In recent years, experimental and numerical research to improve the heat transfer performance, when low conductivity PCM is used, by using some intrusive or non-intrusive strategies have grown dramatically. The strategies such as, active methods (use of agitators, scrappers, vibrators, etc), encapsulation and use of high conductivity *nano*-particles, *lessing* rings, metal matrix, fins, and multiple PCMs. For a comprehensive review on the experimental and numerical studies performed to improve the heat transfer efficiency by enhancing the thermal conductivity of phase change materials (PCMs), reader may refer [6, 7].

In the PCM based storage devices, during the charging and discharging phase, phase-change with very sharp gradients over very small region may occur. In such situations, the intrusive experimental devices of very high response may require and very often experimental techniques could become severely expensive and impossible. Therefore, many researchers focus on the numerical methods in their research works. Numerical study-research on melting and solidification of PCM in various configurations, such as, spherical shells, array of the cylinders, concentric tubes, etc. has been found conducted. References [8, 9], for example, study a spherical shell, [10] studied the laminar flow past an array of in-line cylinders filled with PCM, [11, 12, 13] studied concentric tube thermal storage module, [14] studied the two configurations viz. square external tube and inside circular tube, external circular tube and square tube inside, [15] have studied packed bed of spherical cells, and [16] studied wavy surface filled with PCM containing nano-particles. For a comprehensive review on various PCM modules and heat transfer enhancement strategies, refer to reference [17]. It is observed that a generalized configuration is difficult to ascertain among them as the optimal parameters are often problem dependent. Therefore, there can be many configurations are possible in exploring the phase-change materials. From the literature survey, it is found that a vertical concentric cylindrical PCM module with the gravity assisted flow of heat transfer fluid (H.T.F.) inside of it has not been given suitable attention.

In the present work, 2D unsteady, laminar numerical simulations are performed to compare the three PCMs viz.

pure gallium, paraffin wax, sodium nitrate inside the vertical concentric cylindrical PCM module.

Problem Definitions

Figure 1(a) shows a vertical concentric cylindrical PCM module. In the figure, H.T.F. flows at 590 K in the inner pipe from top to bottom, other surfaces are insulated and a space between concentric cylinders is filled with the PCMs. The variation in the flow variable in the angular direction is assumed to be negligible due to symmetry and a 2D domain (88.9mm × 63.5mm) is considered for the computations, as shown in Fig. 1(b).

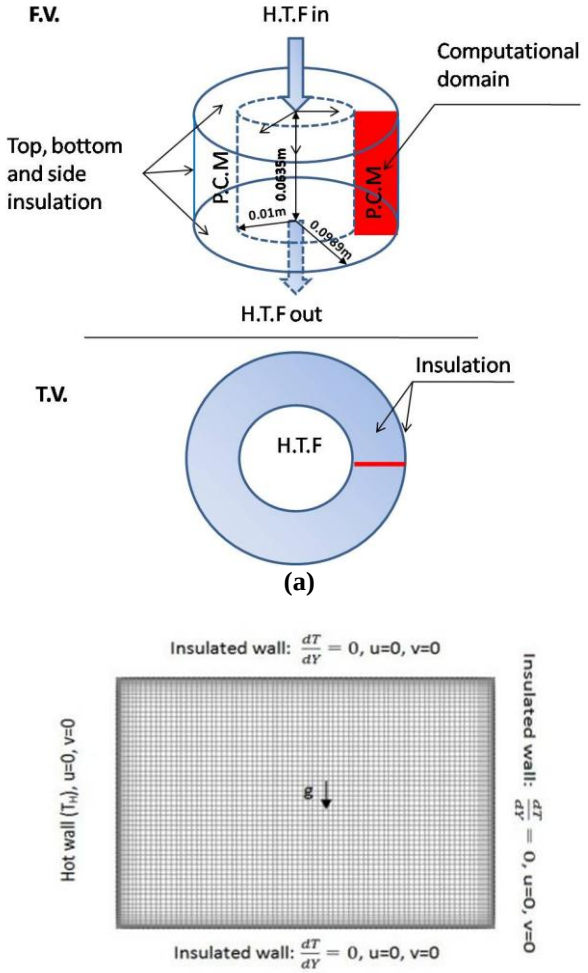

Figure 1: (a) Physical domain of PCM module, (b) Computational domain with boundary conditions

Methodologies

The enthalpy-porosity formulation methodology of ANSYS-Fluent is used with the boundary and initial conditions u =0, v =0 and T =302, 318, 572 K, respectively, for gallium, paraffin wax and sodium nitrate. The conservation equations, in rectangular co-ordinate, governing the two-dimensional, unsteady, laminar flow with constant flow properties are solved. The governing equations considered are:

Continuity equation: $$\frac{\partial u}{\partial x}+\frac{\partial v}{\partial y}=0 \quad (1)$$

Momentum equation:

x-Momentum: $$\frac{\partial u}{\partial t}+u\frac{\partial u}{\partial x}+v\frac{\partial u}{\partial y}=-\frac{1}{\rho}\frac{\partial P}{\partial x}+\nu\left(\frac{\partial^2 u}{\partial x^2}+\frac{\partial^2 u}{\partial y^2}\right)+S_u(u) \quad (2)$$

y-Momentum $$\frac{\partial v}{\partial t}+u\frac{\partial v}{\partial x}+v\frac{\partial v}{\partial y}=-\frac{1}{\rho}\frac{\partial P}{\partial y}+g\beta(T_l-T_f)+\nu\left(\frac{\partial^2 v}{\partial x^2}+\frac{\partial^2 v}{\partial y^2}\right)+S_u(v) \quad (3)$$

where $S_u = A_{mush}(1-\alpha)^2/(\alpha^3+\epsilon)$, $A_{mush} = 10^4$ to 10^7, ϵ is a small number (0.001), $\rho = \rho_{ref}[1-\beta(T-T_{ref})]$, liquid fraction $\alpha = 0$, if $T < T_{solid}$, $\alpha = 1$, if $T > T_{liquid}$ and $\alpha = (T-T_{solid})/(T_{liquid}-T_{solid})$.

Energy equation: $$\frac{\partial H}{\partial t}+u\frac{\partial H}{\partial x}+v\frac{\partial H}{\partial y}=\frac{k}{\rho C_p}\left(\frac{\partial^2 H}{\partial x^2}+\frac{\partial^2 H}{\partial y^2}\right) \quad (4)$$

where, $H = h + \Delta H$, and $h = h_{ref} + \int_{T_{ref}}^{T} C_P T$.

Above governing equations are solved on three grids (90×65, 180×130, 360×260 cells) and three time-steps (0.01, 0.1 and 2) using a SIMPLE algorithm with the second-order upwind scheme for convective and diffusive terms, and the pressure is solved using PRESTO!. For the grid-size and time-step independence and in the subsequent simulations, the convergence criterion for the energy, momentum, and continuity, respectively, is 10^{-6}, 10^{-4} and 10^{-4}. The thermo-physical properties of pure gallium, paraffin wax and sodium nitrate used in the numerical simulation are presented in Table 1.

Table 1: Thermo-physical properties of gallium, paraffin wax and sodium nitrate

	Gallium [18]	**Paraffin wax [19]**	**Sodium nitrate [20]**
Specific heat, J/kg K	381.5	2890	1635
Density, kg/m^3	6088.09	779.73	1903.2
Thermal conductivity, W/m-K	32	0.12	0.5179
Dynamic viscosity, kg/m-s	0.00181	0.002555	0.003150
Latent heat of fusion, J/kg	80160	173400	176256
Solidus temperature (T_{solid}), K	302.93	319	579.15
Liquidus temperature (T_{liquid}), K	302.93	321	579.95
Prandtl number (Pr)	0.0216	61.4125	9.9445
Rayleigh number (Ra)	6×10^5	2.76×10^7	36.695×10^7
Stefan number (Ste)	0.039	4.0833	0.1749

The results of grid-size and time-step independence test are as shown in Figure 2 for all three cases of PCMs i.e. gallium, paraffin wax, and sodium nitrate. It can be noted that, in the absence of the experimental data, grid-size and time-step independence is sufficient criteria for the validation and

verification. Grid size of 180×130 cells and time-step of 0.1s is found to be optimum. The numerical results on the optimal grid size and time step are given in the following section.

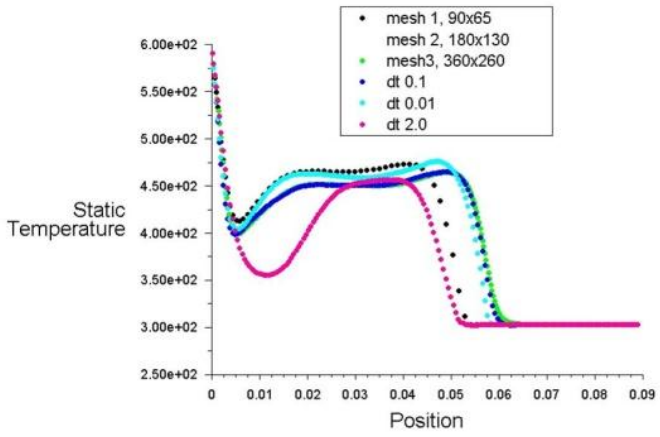

(a) Gallium

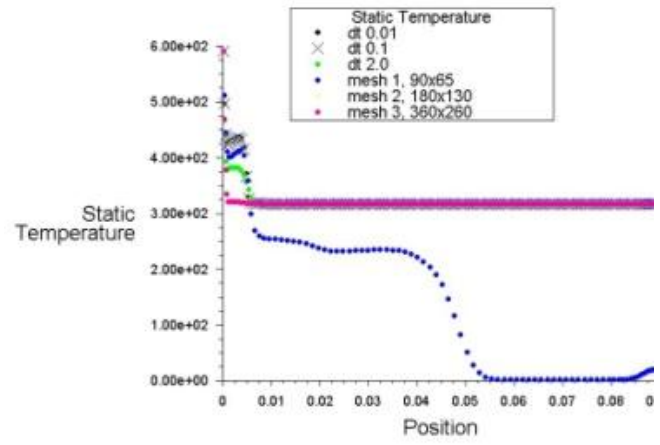

(b) Paraffin wax

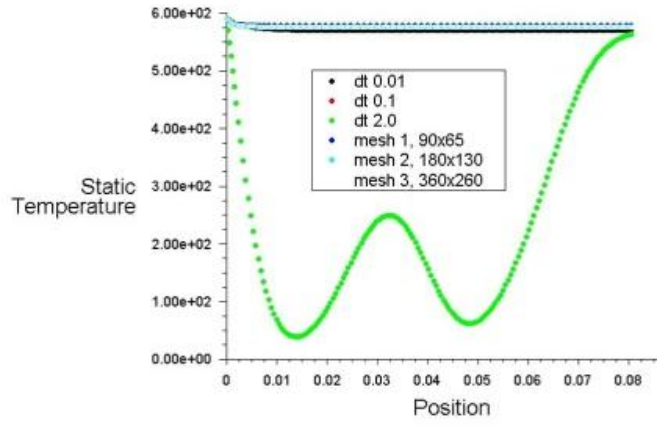

(c) Sodium nitrate

Figure 2: Independence test: Grid-size (Grid-1: 90×65 cells, Grid-2: 180×130 cells, Grid-3: 360×260 cells) at fixed time-step of 0.1 and time-step (0.01, 0.1, 2.0s) at fixed Grid-2

Results and Discussions

The results of 2D, unsteady, and laminar numerical simulations are performed, with same boundary conditions, to compare the three PCMs viz. pure gallium, paraffin wax, sodium nitrate inside the vertical concentric cylindrical PCM module, are presented in this section.

Gallium: Figure 3 shows the contours of liquid mass fraction, temperature and stream function at 10s, 20s, and 30s for the case of gallium PCM. As seen in the figure, that the two rotating cells, in the stream function contours, combines to form one dominant large cell. The convection dominance increases with the time making the interface much curvy than earlier time values during which only conduction is a dominant mode of heat transfer. During conduction dominance (at < 10 sec), the temperature linearly varies with time (see temperature contours). As the melting progresses, at time greater than 10 sec., the conduction and free convection due to buoyancy increases and the temperature gradients are relatively quite high than that of the previous case.

In the contour plots of liquid mass fraction, of Figure 3, the red color indicates liquid PCM and blue color indicates solid PCM. In the beginning, at time < 10 sec, during the melting thermal expansion of the liquid PCM occurs leading to the squeezing of the liquid due to buoyancy force. The squeeziness increases with time and the interface becomes curvier due to the dominance of the natural convection. The reason is that, due to the higher temperature gradients and intensified fluid activity makes the interface more wavy and digressing from top towards the bottom surface.

Paraffin wax: Figure 3 shows temporal evolution of contours of liquid mass fraction, temperature and stream function of paraffin wax PCM. As seen in the figure, that in the beginning, at time < 10 sec, during the melting thermal expansion of the liquid PCM occurs leading to the squeezing of the liquid due to the buoyancy force. The squeezeness increases with time and the morphology of the interface becomes curvier due to the dominance of the free convection. The pattern remains same as observed for the gallium i.e. the intensity of convection increases with time (here, 1 min. onwards). However, the time taken to melt the paraffin wax is very high (i.e. >45 min.) as compared to the case of gallium. This is due to the change in their thermo-physical properties, for example the latent heat of fusion conductivity of the paraffin wax is small (0.12 W/mK) as compared to gallium (32 W/mK). The major temperature gradient occurs in the liquid phase as compared to the solid phase and therefore the thermal conductivity of the liquid phase is the controlling factor for the heat transfer.

From the contours of temperature, in Figure 4, it can be observed that the maximum temperature gradient occurs near the interface at the locations where recirculation (as observed from the contours of stream function) occurs. As against with the previous case of gallium, temperature gradient exits not only in the liquid region but also in the solid region. It means that part of the energy entering from the hot wall is absorbed by the melting front and the part of it by the solid part; in the case of gallium all the energy was absorbed by the interface only.

Sodium nitrate: In Figure 5, the position of the interface, temperature and streamlines at 10, 30, 50, and 85 min are shown. As observed previously, in this case also, for time less than 10 min., the interface is observed to be almost vertical indicating the dominance of the conduction heat transfer. As the free convection fields begin to develop, the intensified convection substantially affects the energy transport from the heated wall. The fluid rising at the hot wall towards the top

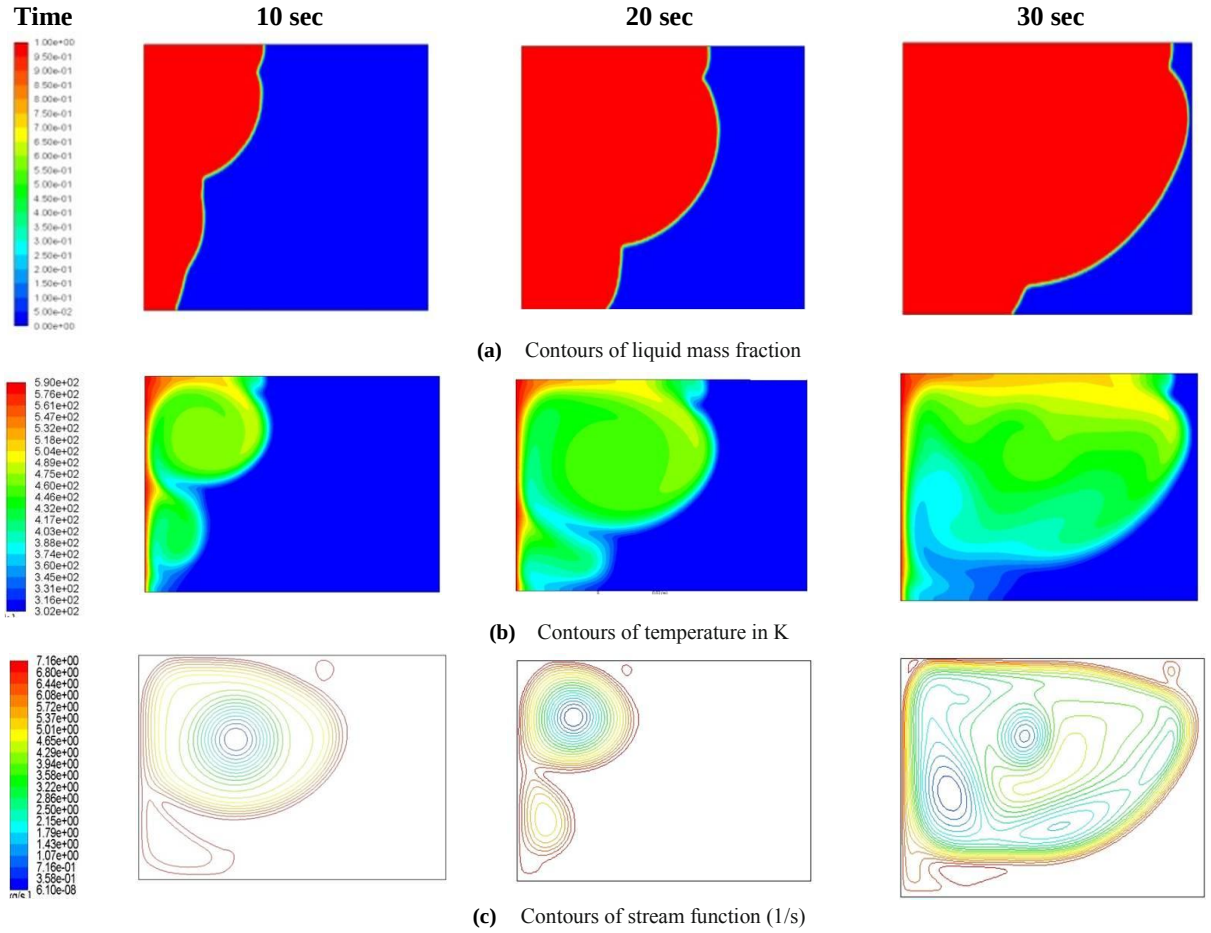

Figure 3: Gallium — Contours of (a) liquid mass fraction, (b) temperature and (c) stream function at various times.

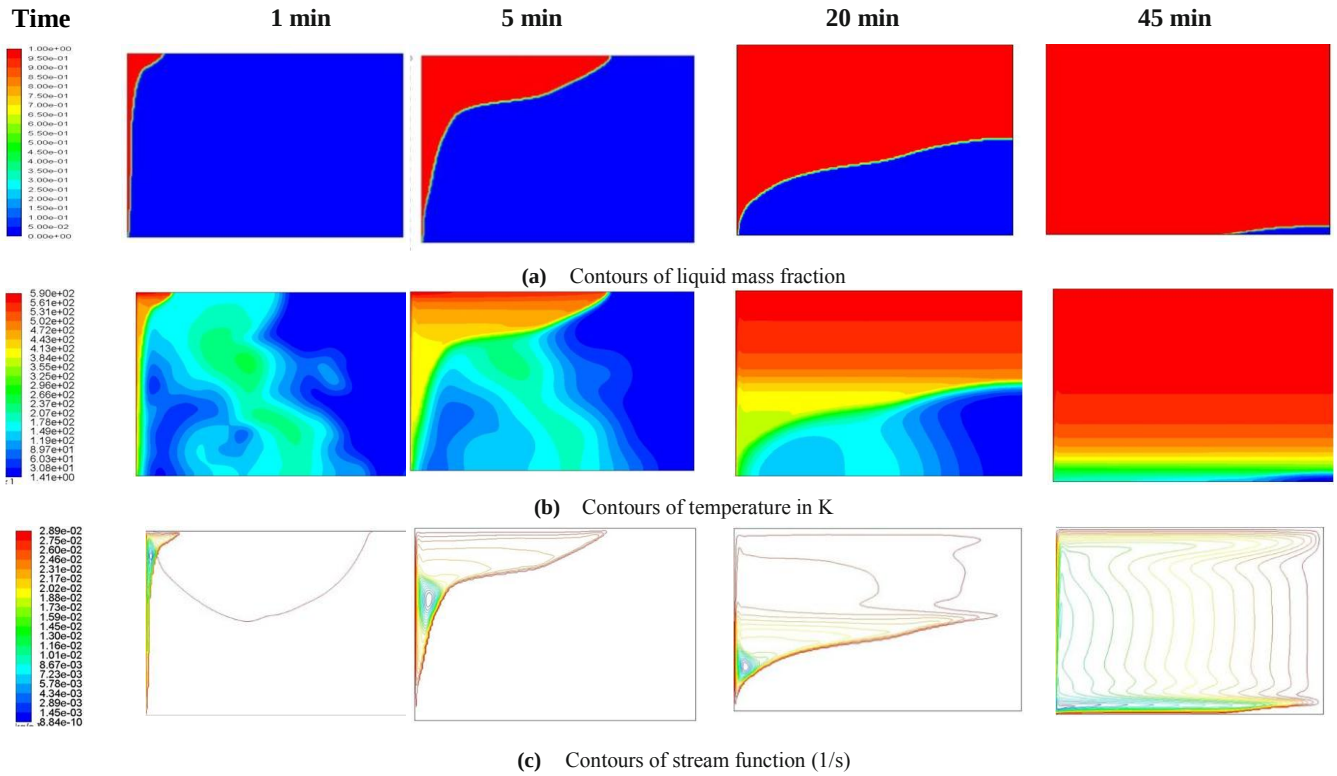

Figure 4: Paraffin wax — Contours of (a) liquid mass fraction, (b) temperature and (c) stream function at various times.

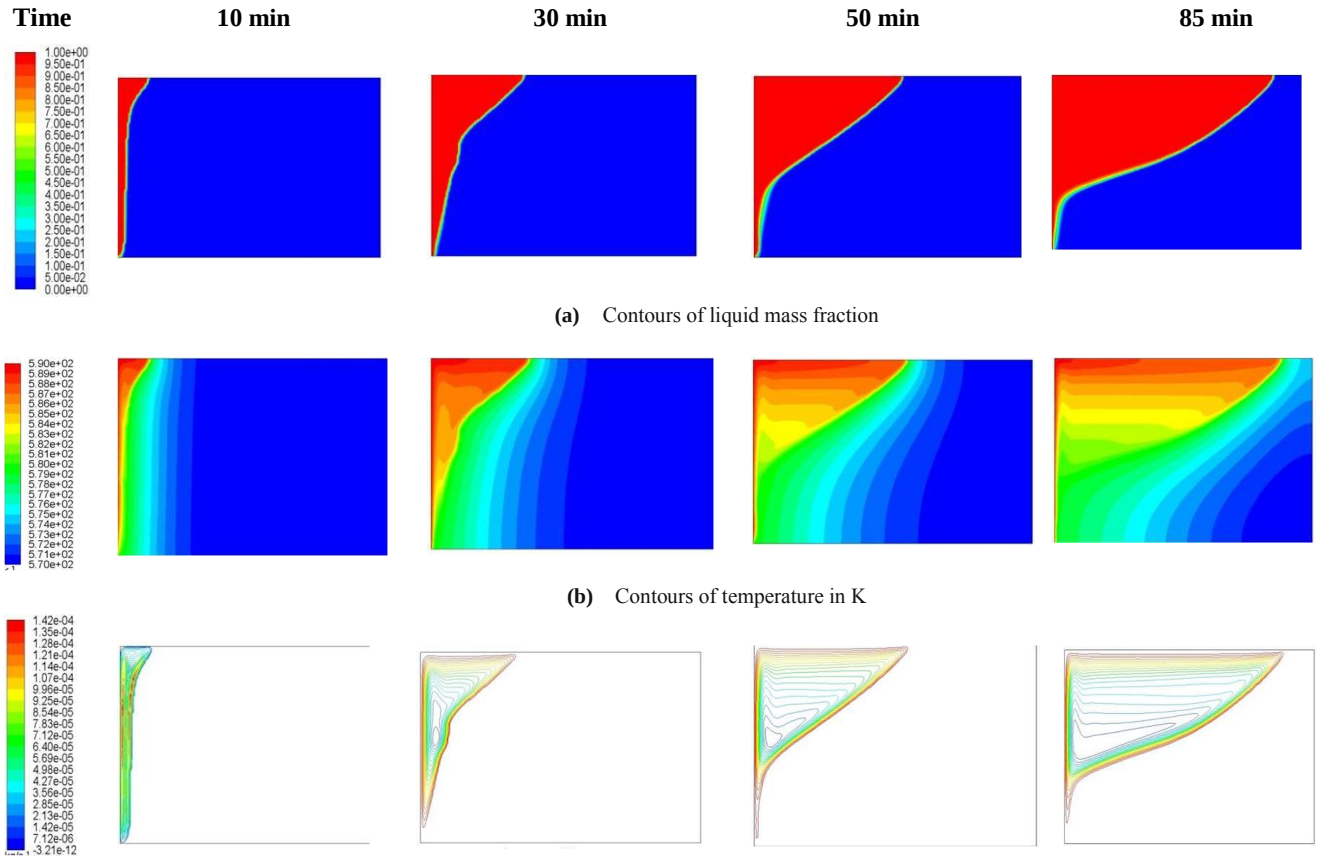

(a) Contours of liquid mass fraction

(b) Contours of temperature in K

(c) Contours of stream function (1/s)

Figure 5: Sodium nitrate — Contours of (a) liquid mass fraction, (b) temperature and (c) stream function at various times.

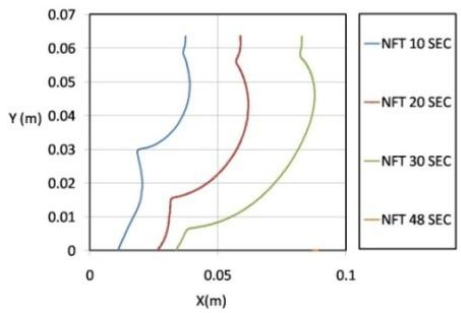

(a) Gallium: Interface locations at various times

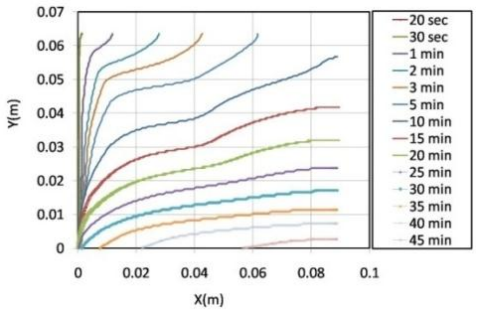

(b) Paraffin wax: Interface locations at various times

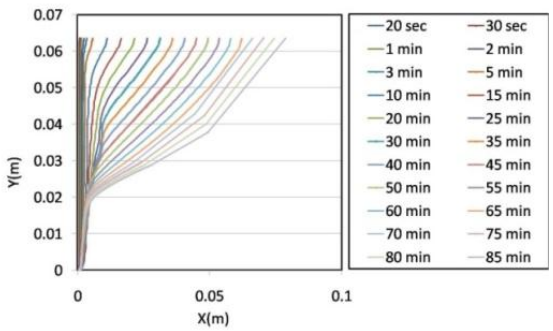

(c) Sodium nitrate: Interface locations at various times

Figure 6: Interface locations at various times: (a) gallium, (b) paraffin wax, (c) sodium nitrate.

wall and hits the solid region nearby, influences the curvature and the speed of advancement of the upper part of the interface, as observed in the previous cases too.

From the comparison of Figure 5 with Figures 3 and 4, the time taken to melt the sodium nitrate is very high. This is attributed to to the change in their thermo-physical properties, for example the latent heat of fusion is relatively high. This may be due to quite higher values of the Rayleigh number (36.695×10^7), indicating the lower value of the thermal diffusivity. From the temperature contours, it is observed, in this case also, that the temperature gradient exits in both the liquid and solid region, as the part of the energy entering from the hot wall, is absorbed by the melting front and part of it by the solid part.

At the top and the bottom walls the interface is more or less straight or perpendicular to the surfaces. However to satisfy the homogeneous Neumann boundary conditions (i.e. zero heat flux) at top and bottom walls, the interface must be normal to the surfaces. This observation can be attributed to the fact that the small secondary re-circulating fluid is present near the bottom and top walls.

Interface locations and the average Nusselt number: Figure 6 shows the temporal evolution of the interface inside the rectangular cavity filled with three PCMs. It can be seen from the figure that the interface becomes curvy at later times due to the intensified convection activities.

Figure 6 show the averaged Nussel number as a function of time at the hot wall of the cavity for three PCMs. Here, the averaged Nusselt number is calculated as $(\mathrm{Nu})_{\mathrm{avg}} = (\mathrm{q}' \cdot \Delta\mathrm{Y})/(\Delta\mathrm{T} \cdot \mathrm{k})$ where q' is the heat flux, and $\Delta\mathrm{Y}$ is the change in length at the point of estimation, and $\Delta\mathrm{T}$ is the temperature change with the reference temperature and k is the thermal conductivity of fluid. It can be observed that, due to change in the thermo-physical properties, the averaged Nusselt number is high for the lower thermal conductivity fluids.

Conclusions

2D, unsteady, and laminar numerical simulations are performed, with same boundary conditions, to compare the three PCMs viz. pure gallium, paraffin wax, sodium nitrate inside the vertical concentric cylindrical PCM module, are presented in this section. The model is sufficiently validated and verified using the grid-size and time-step independence. The numerical comparison between metal-based, organic and inorganic compound-based PCM is made on optimal grid and at optimum time step. The result indicates the dominance of free convection in all the cases. However, the morphology of the interface and the temporal response is quite different in the cases of gallium, paraffin wax and the sodium nitrate, due to variations in their thermo-physical properties. Among them, the sodium nitrate is sluggish in its response and its efficiency should be enhanced looking at its ease in availability and the cost. In the future simulations, the heat transfer enhancement strategies could be tested for sodium nitrate PCM.

References

[1] S. Y. Kee, Y. Munusamy, and K. S. Ong, "Review of solar water heaters incorporating solid-liquid organic phase change materials as thermal storage", *Applied Thermal Engineering*, vol. **131**, 455–471, 2018.

[2] J. Jaguemont, N. Omar, P. V. Bossche, J. Mierlo, "Phase-change materials (PCM) for automotive applications: A review", *Applied Thermal Engineering* vol. **132**, 308–320, 2018.

[3] V. Reddy, V. Mudgal, and T. K. Mallick, "Review of latent heat thermal energy storage for improved material stability and effective load management", *Journal of Energy Storage*, vol. **15**, 205–227, 2018.

[4] A. Sharma, V. V. Tyagi, C. R. Chen, D. Buddhi, "Review on thermal energy storage with phase change materials and applications", *Renewable and Sustainable Energy Reviews*, vol. **13**, 318–345, 2009.

[5] J. Kosny, N. Shukla, and A. Fallahi, "Cost Analysis of Simple Phase Change Material-Enhanced Building Envelopes in Southern U.S. Climates; Office of Energy Efficiency and Renewable Energy: Denver, CO, USA, 2013.

[6] L. Fan, and J. M. Khodadadi, "Thermal conductivity enhancement of phase change materials for thermal energy storage: A review", *Renewable and Sustainable Energy Reviews*, vol. **15**, 24–46, 2011.

[7] M. Liu, W. Saman, and F. Bruno, "Review on storage materials and thermal performance enhancement techniques for high temperature phase change thermal storage systems", *Renewable and Sustainable Energy Reviews,* vol. **16**, 2118–2132, 2012.

[8] E. Assis, L. Katsman, G. Ziskind, and R. Letan, "Numerical and experimental study of melting in a spherical shell", *Int. J. Heat Mass Tran.*, vol. **50**, 790–1804, 2007.

[9] S. F. Hosseinizadeh, A. A. Rabienataj Darzi, and F. L. Tan, "Numerical investigations of unconstrained melting of nano-enhanced phase change material (NEPCM) inside a spherical container", *Int. J. Therm. Sci.*, vol. **51**, 77–83, 2012.

[10] E. M. Alawadhi, "Thermal analysis of transient laminar flow past an in-line cylinders array containing phase change material", *Proc. IMechE A J. Power Energ.*, vol. **223(4)**, 349–360, 2009.

[11] G. H. Bagheri, M. A. Mehrabian, and K. Hooman, "Numerical study of the transient behaviour of a thermal storage module containing phase-change material", *Proc. IMechE A J. Power Energ.*, vol. **224(4)**, 349–360, 2010.

[12] K. W. Ng, Z. X. Gong, and A.S. Mujumdar, "Heat transfer in free convection-dominated melting of phase change material in horizontal annulus", *Int. Comm. Heat Mass Tran.*, vol. **25(5)**, 631–640, 1998.

[13] O. Mesalhy, K. Lafdi, A. Elgafy, and K. Bowman, "Numerical study for enhancing the thermal conductivity of the phase change material (PCM) storage using high thermal conductivity porous matrix", *Energy Convers. Manag.*, vol. **46**, 847–867, 2005.

[14] D. B. Khillarkar, Z. X. Gong, and A. S. Mujumdar, "Melting of a phase change material in concentric horizontal annuli of arbitrary cross-section", *Appl. Therm. Eng.*, vol. **20**, 893–912, 2000.

[15] A. F. Regin, S. C. Solanki, and J. S. Saini, "An analysis of a packed bed latent heat thermal energy storage system using PCM capsules: numerical investigation", *Renew Energy*, vol. **34(7)**, 1765–73, 2009.

[16] M. Abdollahzadeh, and M. Esmaeilpour, "Enhancement of phase change material (PCM) based latent heat storage system with nano fluid and wavy surface", *Int. J. Heat Mass Tran.,* vol. **80**, 376–385, 2015.

[17] J. P. D. Cunha, and P. Eames, "Thermal energy storage for low and medium temperature applications using phase change materials – A review", *Applied Energy*, vol. **177**, 227–238, 2016.

[18] A. D. Brent, V. R. Voller, and K. T. J. Reid, "Enthalpy-porosity technique for modeling convection-diffusion phase change: application to the melting of a pure metal", *Numerical Heat Transfer, Part A Applications*, vol. **13(3)**, 297-318 (1988)

[19] R. Kandasamy, X. Q. Wang, and A. S. Mujumdar, "Transient cooling of electronics using phase change material (PCM)-based heat sinks", *Applied Thermal Engineering*, vol. **28**, 1047–1057, 2008.

[20] A. Keshavarz, M. Ghassemi, and A. Mostafavi, "Thermal Energy Storage Module Design Using Energy and Exergy Analysis", *Heat Transfer Engineering*, vol. **24(3)**, 76-85, 2003.